International Journal of Theoretical Physics, Vol. 38, No. 3, 1999

Anisotropic Heisenberg Magnet with Long-Range Interactions. Integrability and Phase Structure

Vahid Karimipour[1,2] and Mohammad Khorrami[1,2,3]

Received July 20, 1998

We show that the *xxz* Heisenberg magnet with long-range interactions in a magnetic field, is integrable both classically and quantum mechanically. Explicit expressions are given for the involutive integrals of the motion. The nature of the spectrum and the ground state are clarified and the partition function is calculated exactly in the thermodynamic limit. A detailed study of the phase structure of the system is also performed.

1. INTRODUCTION

The last two decades have witnessed an upsurge of interest in and intensive study of integrable systems, in classical and quantum 1 + 1-dimensional field theories, in quantum spin chains and their generalizations, and also in 2-dimensional statistical mechanical models (see refs. 1–3 for reviews and further references). Investigation of this area, besides paving the way for generalizations to higher dimensions, has revealed many beautiful mathematical structures, which lie behind the notion of integrability. On the physical side, the study of integrable models, especially in statistical mechanics, has deepened our knowledge of phase transitions in two dimensions. As far as quantum lattice systems with local interactions are concerned, the R-matrix formalism and the associated algebraic Bethe ansatz has turned into a paradigm for exactly solvable models. The most famous examples of this type are the isotropic and anisotropic Heisenberg chains, which have su(2) and $su_q(2)$ symmetries, respectively. The systems referred to above have local

[1] Department of Physics, Sharif University of Technology, P.O. Box 9161, Tehran 11365, Iran.
[2] Institute for Studies in Theoretical Physics and Mathematics, P.O. Box 5531, Tehran 19395, Iran; e-Mail: vahid@netware2.ipm.ac.ir, mamwad@netware2.ipm.ac.ir.
[3] Institute for Advanced Studies in Basic Sciences, P.O. Box 159, Gava Zang, Zanjan 45195, Iran.

0020-7748/99/0300-097 1$16.00/0

interactions. Other systems with long-range inverse-square or inverse-sine-squared interactions have also been studied intensively [4–6]. The system we study in this paper is much simpler than those described above, and although a problem as simple as the one we are concerned with may have been well studied by various means, we have preferred to look at this problem from the view of integrable systems and see how far the knowledge of integrability allows one to proceed in determination of the exact properties of this system. It is the aim of the present paper to study a system of N spins interacting with each other (with equal coupling) and with an external magnetic field.

2. CLASSICAL INTEGRABILITY

The system under consideration consists of N vectors $\mathbf{S}_i$ ($i = 1,2,\ldots,N$), interacting by the Hamiltonian

$$H = -\frac{J}{N}\sum_{i,j} \mathbf{S}_i \cdot \mathbf{S}_j - \frac{A}{N}\sum_{i,j} S_i^z S_j^z - B\sum_i S_i^z \tag{1}$$

with the Poisson brackets

$$\{S_i^a, S_j^b\} = \epsilon_c^{ab}\delta_{ij}S_i^c \tag{2}$$

Here J is a real parameter (not necessarily positive) and the parameters A and B control the anisotropy and the strength of the magnetic field, respectively. In Eq. (2) and in the rest of the paper, a contraction between an upper and a lower index means summation over that index. To show that this system describes an integrable dynamical system in the Liouville sense, we define the global variables [7]

$$X_m^a = \sum_{i=1}^{m} S_i^a \tag{3}$$

It is now easily verified that the new dynamical variables satisfy the Poisson brackets

$$\{X_m^a, X_n^b\} = \epsilon_c^{ab} X_{(m,n)}^c \tag{4}$$

where (m, n) denotes the minimum of m and n. In fact, for each fixed n, the variables X_n^a satisfy among themselves the Poisson brackets pertaining to the Lie algebra su(2). Constructing for each copy the Casimir function

$$C_m = \delta_{ab} X_m^a X_m^b \tag{5}$$

we obtain

$$\{C_m, X_n^b\} = 2\epsilon^b_{ac} X^a_m X^c{}_{(m,n)} \tag{6}$$

which means that the Casimir function of one copy of the algebra has nontrivial Poisson bracket with the coordinate variables of other copies. Despite this fact, one obtains after a simple calculation the following result:

$$\{C_m, C_n\} = 4\epsilon_{abc} X^a_m X^b_n X^c_{(m,n)} = 0 \tag{7}$$

Furthermore, from (6) one obtains that all the Casimir functions Poisson commute with the coordinate variables $X^a_N := (X_N, Y_N, Z_N)$:

$$\{C_m, X_N^b\} = 2\epsilon^b_{ac} X^a_m X^c_m = 0 \tag{8}$$

We also note that the Hamiltonian (1) can be written compactly as

$$H = -\frac{J}{N} C_N - \frac{A}{N} Z_N^2 - BZ_N \tag{9}$$

From (7) and (8), we obtain that the functions $C_2, C_3, \ldots, C_N$, and Z_N are N integrals of motion in involution with each other, and the Hamiltonian is a function of these integrals. Note that the function C_1 should not be counted among the integrals of motion. The above analysis proves the integrability of the system in the classical case.

3. QUANTUM INTEGRABILITY

We now consider the quantum version of the model, where the variables $\mathbf{S}_i$ are replaced by the operators $\hat{\mathbf{S}}_i$ acting on the Hilbert space $\mathcal{H} = h^{\otimes N}$. The local Hilbert space at each site carries the spin-j representation of the su(2) algebra, and the local operators $\hat{\mathbf{S}}_i$ act nontrivially only on the ith site:

$$\hat{S}^a_i = 1 \otimes 1 \ldots 1 \otimes \hat{S}^a \otimes 1 \ldots 1 \otimes 1 \tag{10}$$

The Poisson brackets (2) are replaced by the su(2) Lie brackets:

$$[\hat{S}^a_i, \hat{S}^b_j] = i\epsilon^{ab}_c \hat{S}^c_j \delta_{ij} \tag{11}$$

The global operators $\hat{\mathbf{X}}_n$ are defined as in (3):

$$\hat{X}^a_m = \sum_{n=1}^{m} \hat{S}^a_i \tag{12}$$

with the commutation relations

$$[\hat{X}^a_m, \hat{X}^b_n] = i\epsilon^{ab}_c \hat{X}^c_{(m,n)} \tag{13}$$

Straightforward calculations now lead to the following result:

$$[\hat{C}_m, \hat{X}_n^b] = 2\epsilon_{ac}^{b}(\hat{X}_m^a \hat{X}_{(m,n)}^c + \hat{X}_{(m,n)}^c \hat{X}_m^a) \tag{14}$$

from which we obtain

$$[\hat{C}_m, \hat{C}_n] = i\epsilon_{abc}\{\hat{X}_n^b[\hat{X}_m^a \hat{X}_{(m,n)}^c + \hat{X}_{(m,n)}^c \hat{X}_m^a] + [\hat{X}_m^a \hat{X}_{(m,n)}^c + \hat{X}_{(m,n)}^c \hat{X}_m^a]\hat{X}_n^b\} \tag{15}$$

For definiteness, let us take $m < n$. Then the index (m, n) is equal to m and the expression in the brackets is obviously symmetric under the interchange of a and c, so that it gives zero when contracted with ϵ_{abc}. Therefore we have

$$[\hat{C}_m, \hat{C}_n] = 0 \tag{16}$$

Furthermore, from (14) we obtain

$$[\hat{C}_m, \hat{X}_n^b] = 0, \qquad m \leq n \tag{17}$$

In particular, all the Casimirs commute with the operators $\hat{\mathbf{X}}_N$:

$$[\hat{C}_m, \hat{X}_N^a] = 0, \qquad \forall m \tag{18}$$

The collection of the operators $C_2, C_3, \ldots, C_N$, and $Z_N = X_N^3$ are N commuting operators and the Hamiltonian can be expressed in terms of these operators as in (9). This proves the quantum integrability of the system, for any spin.

4. THE SPECTRUM

In the rest of the paper we restrict ourselves to the spin-1/2 representation. The integrable structure of the model allows us to construct the simultaneous eigenstates of the operators H, $C_2, \ldots, C_N$, and Z_N. Denoting these states by $\Psi_{j_1,j_2,\ldots,j_N,m_N}$, we have

$$\hat{C}_k\Psi_{j_1,j_2,\ldots,j_N,m_N} = j_k(j_k + 1)\Psi_{j_1,j_2,\ldots,j_N,m_N} \tag{19}$$

$$\hat{Z}_N\Psi_{j_1,j_2,\ldots,j_N,m_N} = m_N\Psi_{j_1,j_2,\ldots,j_N,m_N} \tag{20}$$

and

$$\hat{H}\Psi_{j_1,j_2,\ldots,j_N,m_N} = \left[-\frac{J}{N}j_N(j_N + 1) - \frac{A}{N}m_N^2 - Bm_N \right]\Psi_{j_1,j_2,\ldots,j_N,m_N} \tag{21}$$

The subspaces

$$\epsilon_{j_2,j_3,\ldots,j_N} := \{\Psi_{j_1,j_2,\ldots,j_N,m_N} | m_N = -j_N, \ldots, j_N\}$$

are in one-to-one correspondence with the paths on the Bratelli diagram for the su(2) algebra (Fig. 1). Each path in the diagram corresponds to a definite pattern of fusion and reduction of su(2) representations on the consecutive sites of the lattice. If N is even, the leftmost path corresponds to the one-dimensional eigenspace $\epsilon_{0,1/2,0,1/2,0,\ldots,1/2,0}$, and if N is odd, it corresponds to the two-dimensional eigenspace $\epsilon_{0,1/2,0,1/2,0,\ldots,1/2}$. The rightmost path always corresponds to the $\frac{1}{2}N(\frac{1}{2}N + 1)$-dimensional eigenspace $\epsilon_{1,3/2,2,\ldots,N/2}$.

Next, we need the multiplicity of the representation with $j_N = S$ in the tensor product of N spin-1/2's. This is equal to the number of paths beginning at the top of the Bratelli diagram and ending at the point of spin S at the Nth level. They can be easily calculated as follows: Consider Fig. 2. This is a modified version of Pascal's triangle. It is easy to see that that part of this triangle which is inside the dashed lines denotes the required multiplicities. The numbers written in the triangle obey the same rule as those in Pascal's triangle, namely each number is the sum of two numbers in the upper row adjacent to it. The only difference is in the boundary conditions of this triangle. In Pascal's triangle, the sides of the triangle are both equal to 1, whereas here the left side is equal to -1. Our aim is now to calculate the

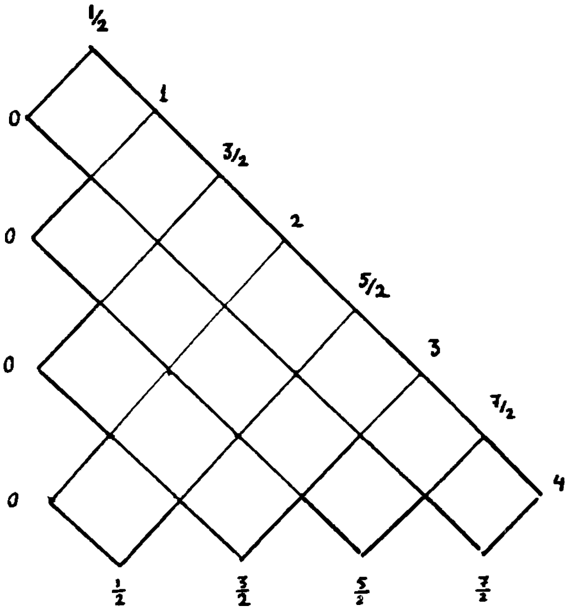

Fig. 1. The Bratelli diagram for su(2) algebra.

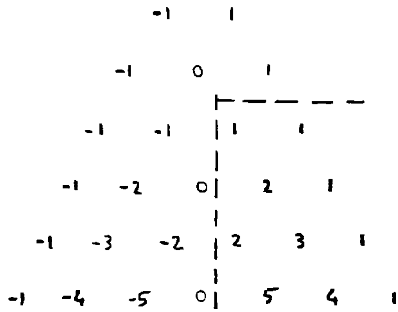

Fig. 2. A modified Pascal triangle.

numbers of this triangle, which are denoted by $g(N, S)$. Here N is the number of the row (starting from $N = 1$ in the second row), and $S = N/2 - k$, where k is an integer, which is equal to zero at the right side and increases by one each time we go one step toward the left.

However, as the recursion relation determining g is linear, g can be written as

$$g(N, S) = g_1(N, S) - g_2(N, S) \tag{22}$$

where g_1 and g_2 are the solutions of the same recursive equation with different boundary conditions. The boundary condition for g_1 is zero at the left side and one at the right side; that of g_2 is the reverse. It is easy to see that with these boundary conditions, g_1 and g_2 are in fact coefficients of the binomial expansion, that is,

$$\begin{aligned} g_1(N, S) &= \binom{N}{N/2 - S} \\ g_2(N, S) &= \binom{N}{N/2 + S + 1} \end{aligned} \tag{23}$$

So, one obtains

$$g(N, S) = \binom{N}{N/2 - S} \frac{2S + 1}{N/2 + S + 1} \tag{24}$$

This expression gives the degeneracy of all the energy levels. With these preparations we will be able to calculate exactly the partition function of the system in the thermodynamic limit.

5. STATISTICAL PROPERTIES OF THE SYSTEM

Our next task is to calculate the partition function corresponding to the Hamiltonian (1). This is

$$
\begin{aligned}
Z &= \sum_{S=0,1/2}^{N/2} \sum_{M=-S}^{S} g(N, S) \exp\left\{\beta\left[J \frac{S(S+1)}{N} + A \frac{M^2}{N} + BM\right]\right\} \\
&= \sum_{S=0,1/2}^{N/2} \sum_{M=-S}^{S} g(N, S) \exp\left\{N\beta\left[J\zeta\left(\zeta + \frac{1}{N}\right) + A\mu^2 + B\mu\right]\right\}
\end{aligned}
\tag{25}
$$

where S is the total spin of the system, M is the magnetization of the system, i.e., the third component of the spin, and ζ and μ are the densities corresponding to S and M, respectively: $\zeta := S/N$ and $\mu := M/N$. In the thermodynamic limit, the sum is determined by its largest term. Using the Stirling approximation for $N!$, and denoting βJ, βA, and βB by j, a, and b, respectively, we have

$$
\begin{aligned}
Z &= \sum_S \sum_M \exp\left\{N\left[j\zeta^2 + a\mu^2 + b\mu - \left(\frac{1}{2} - \zeta\right)\ln\left(\frac{1}{2} - \zeta\right)\right.\right. \\
&\qquad \left.\left. - \left(\frac{1}{2} + \zeta\right)\ln\left(\frac{1}{2} + \zeta\right) + O\left(\frac{1}{N}\right)\right]\right\} \\
&=: \sum_S \sum_M \exp[Nu(\zeta, \mu)]
\end{aligned}
\tag{26}
$$

A detailed analysis of the maxima of the function $u(\zeta, \mu)$ depending on the value of the parameters is now in order. We assume, without loss of generality, that $b \geq 0$. Two cases may happen.

Case 1. a is nonnegative. Here $u(\zeta, \mu)$ attains its maximum at $\mu = \zeta$, which means that the total spin aligns itself in the direction of the magnetic field and there is no quantum fluctuation in the components of the magnetization perpendicular to the magnetic field. Denoting by $\tilde{u}(\zeta)$ the value of $u(\zeta, \bar{\mu})$ where $\bar{\mu}$ maximizes $u(\zeta, \mu)$, we have

$$
\begin{aligned}
Z &= \sum_S \exp[N\tilde{u}(\zeta)] \\
&= \sum_S \exp\left\{N\left[(j + a)\zeta^2 + b\zeta\right.\right. \\
&\qquad \left.\left. - \left(\frac{1}{2} - \zeta\right)\ln\left(\frac{1}{2} - \zeta\right) - \left(\frac{1}{2} + \zeta\right)\ln\left(\frac{1}{2} + \zeta\right)\right]\right\}
\end{aligned}
\tag{27}
$$

To find the value of the magnetization ζ which maximizes $\tilde{u}(\zeta)$, we set

$$\frac{d\tilde{u}}{d\zeta} = 2(j + a)\zeta + b + \ln\frac{1 - 2\zeta}{1 + 2\zeta} \tag{28}$$

An analysis of this equation reveals the following values for ζ depending on the value of the magnetic field b and the parameter $j + a$:

1a. Nonzero magnetic field ($b > 0$). In this case the equation

$$\frac{d\tilde{u}}{d\zeta} = 0 \tag{29}$$

has only one solution for ζ, which is between 0 and 1/2.

1b. Zero magnetic field, $b = 0$. In this case, zero is always a solution for ζ. However, if $j + a > 2$, this value of ζ leads to a minimum for $\tilde{u}$. In this case, there is another solution, which is between 0 and 1/2, and makes $\tilde{u}$ maximum, so that we have to consider two more subcases:

1b1. $j + a < 2$. This yields

$$\zeta = 0 \tag{30}$$

1b2. $j + a > 2$. In this case, ζ is the nonzero solution of (29).

Case 2. a is negative. In this case the value $\bar{\mu}$ at which $u(\zeta, \mu)$ takes its maximum depends on ζ:

$$\bar{\mu} = \begin{cases} -b/(2l;a), & -b/(2a) < \zeta \\ \zeta, & -b/(2a) > \zeta \end{cases} \tag{31}$$

and

$$\tilde{u}(\zeta) = \begin{cases} j\zeta^2 - \dfrac{b^2}{4a} - \left(\dfrac{1}{2} - \zeta\right)\ln\left(\dfrac{1}{2} - \zeta\right) - \left(\dfrac{1}{2} + \zeta\right)\ln\left(\dfrac{1}{2} + \zeta\right), & -\dfrac{b}{2a} < \zeta \\ (j + a)\zeta^2 + b\zeta - \left(\dfrac{1}{2} - \zeta\right)\ln\left(\dfrac{1}{2} - \zeta\right) - \left(\dfrac{1}{2} + \zeta\right)\ln\left(\dfrac{1}{2} + \zeta\right), & -\dfrac{b}{2a} > \zeta \end{cases} \tag{32}$$

which leads to

$$\frac{d\tilde{u}}{d\zeta} = \begin{cases} 2j\zeta + \ln\dfrac{1 - 2\zeta}{1 + 2\zeta}, & -\dfrac{b}{2a} < \zeta \\ 2(j + a)\zeta + b + \ln\dfrac{1 - 2\zeta}{1 + 2\zeta}, & -\dfrac{b}{2a} > \zeta \end{cases} \tag{33}$$

If $\bar{\zeta} = -b/(2a)$, we have

$$-\frac{jb}{a} + \ln \frac{1 + b/a}{1 - b/a} = 0 \tag{34}$$

We then have to consider the following subcases:

2a. $j > (a/b) \ln [(1 + b/a)/(1 - b/a)]$. In this case, $\bar{\zeta}$ is the nonzero solution of the equation

$$2j\bar{\zeta} + \ln \frac{1 - 2\bar{\zeta}}{1 + 2\bar{\zeta}} = 0 \tag{35}$$

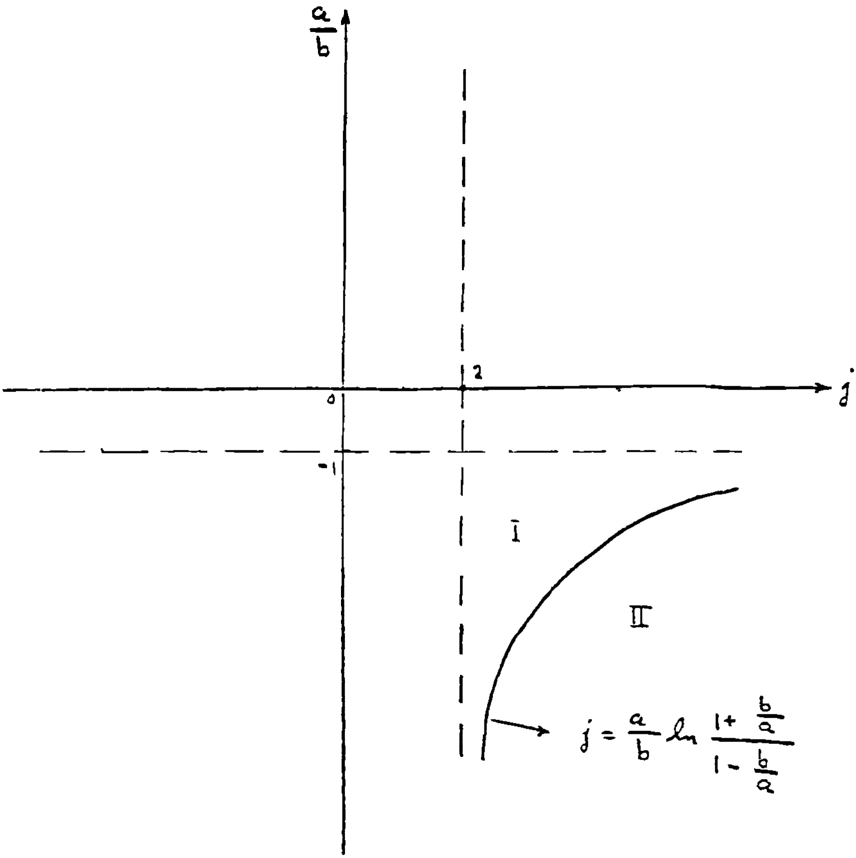

Fig. 3. Phase diagram for $b > 0$.

2b. $j \leq (a/b)\ln[(1+b/a)/(1-b/a)]$. Here $\bar{\zeta}$ is the solution of

$$2(j+a)\bar{\zeta} + b + \ln\frac{1-2\bar{\zeta}}{1+2\bar{\zeta}} = 0 \tag{36}$$

To summarize, in the general case $b > 0$, there are two regions I and II in Fig. 3, and we have

$$\begin{cases} (\bar{\zeta} > 0, \text{ depending on } j,\ a, \text{ and } b;\ \bar{\mu} = \bar{\zeta}), & \text{I} \\ (\bar{\zeta} > 0, \text{ depending only on } j;\ \bar{\mu} = -b/(2a)), & \text{II} \end{cases} \tag{37}$$

If $b = 0$, the region I splits into two subregions. In this case, it is better to work in the j–a plane (Fig. 4). We have

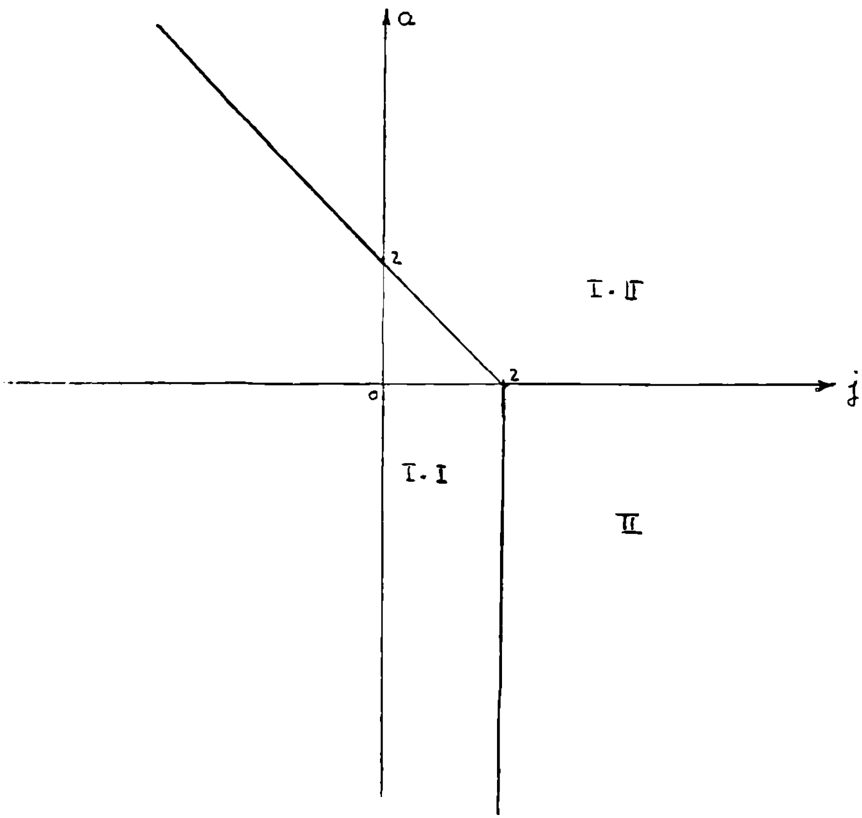

Fig. 4. Phase diagram for $b = 0$.

$$\begin{cases} (\bar{\zeta} = 0;\ \bar{\mu} = 0, & \text{I.I} \\ (\bar{\zeta} > 0,\ \text{depending on } j \text{ and } a;\ \bar{\mu} = \bar{\zeta}), & \text{I.II} \\ (\bar{\zeta} > 0,\ \text{depending only on } j;\ \bar{\mu} = 0), & \text{II} \end{cases} \tag{38}$$

6. PHASE DIAGRAMS OF THE SYSTEM

We now consider the phase diagrams of the system using the two control parameters B and T. Figures 5–7 show the isomagnetic fields, and Figs. 8–10 show the isotherms of the system.

Figure 5, in which $J > 0 > A$, shows a transition curve, qsr. For $B > -A$, the magnetization is parallel to the magnetic field. For $B < -A$, the magnetization is parallel to the magnetic field at high temperatures. But at a certain temperature the component of the magnetization parallel to the magnetic field becomes constant and the total magnetization itself becomes B independent. This phase transition corresponds to a transition from region I to region II in Fig. 3. There is a spontaneous magnetization for $kT < J/2$.

Figure 6, in which $J, J + A < 0$, shows a transition at zero temperature: for $B > -J - A$, the zero-temperature magnetization is 1/2. For magnetic fields less than that, it is less than 1/2. The magnetization is always parallel to the magnetic field. There is no spontaneous magnetization.

Figure 7, in which $A, J + A > 0$, shows a spontaneous magnetization for $kT < (J + A)/2$. The magnetization is always parallel to the magnetic field.

Figure 8, in which $J > 0 > A$, shows a transition curve, ors. For $kt > J/2$, the magnetization is parallel to the magnetic field, and there is no

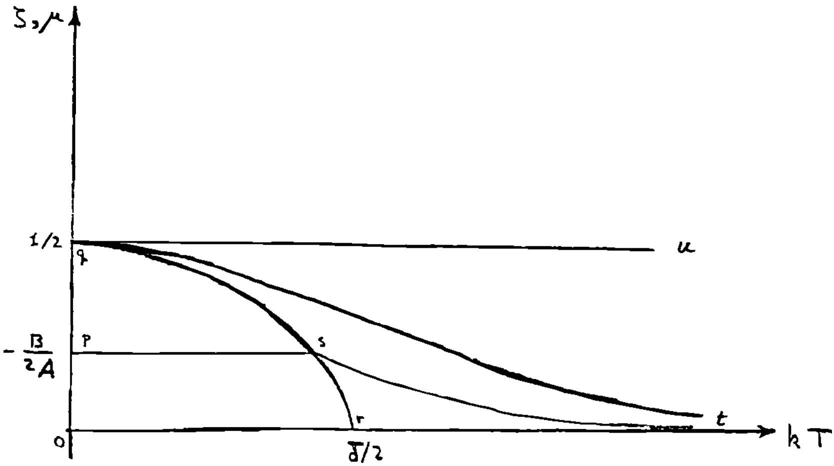

Fig. 5. Isomagnetic fields for $J > 0 > A$. qu: μ and ζ for $B \to \infty$. qt: μ and ζ for $B = -A$. qst: ζ for $0 < B < -A$. pst: μ for $0 < B < -A$. qsrt: ζ for $B = 0$. ort: μ for B = 0.

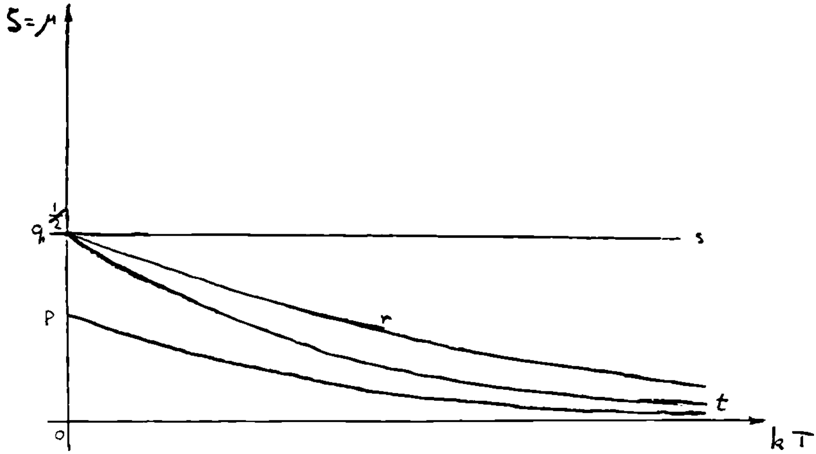

Fig. 6. Isomagnetic fields for J, $J + A < 0$. qs: μ and ζ for $B \to \infty$. qrt: μ and ζ for $B > -J - A$. qt: μ and ζ for $B = -J - A$. pt: μ and ζ for $0 < B < -J - A$. ot: μ and ζ for $B = 0$.

spontaneous magnetization. For $kT < J/2$, the magnetization is parallel to the magnetic fields at high fields. But at a certain magnetic field the component of the magnetization parallel to the magnetic field becomes proportional to the magnetic field and T independent; the total magnetization becomes constant. This phase transition corresponds to a transition from region I to region II in Fig. 3.

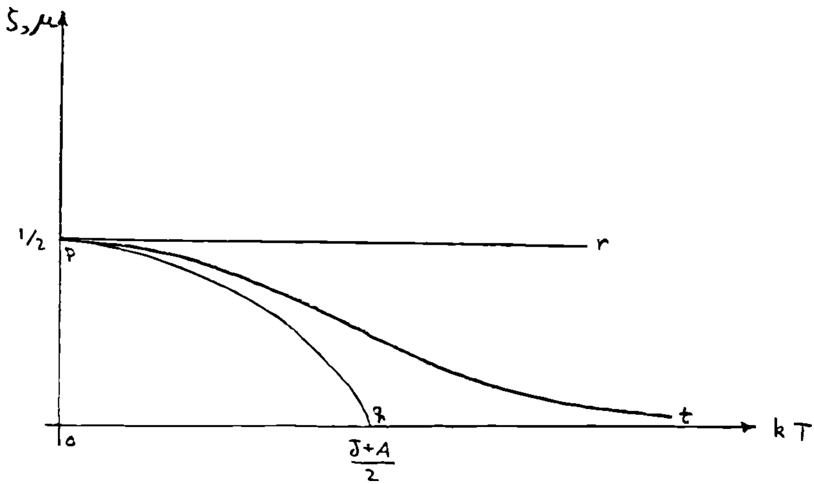

Fig. 7. Isomagnetic fields for A, $J + A > 0$. pr: μ and ζ for $B \to \infty$. pt: μ and ζ for $0 < B$. pqt: μ and ζ for $B = 0$.

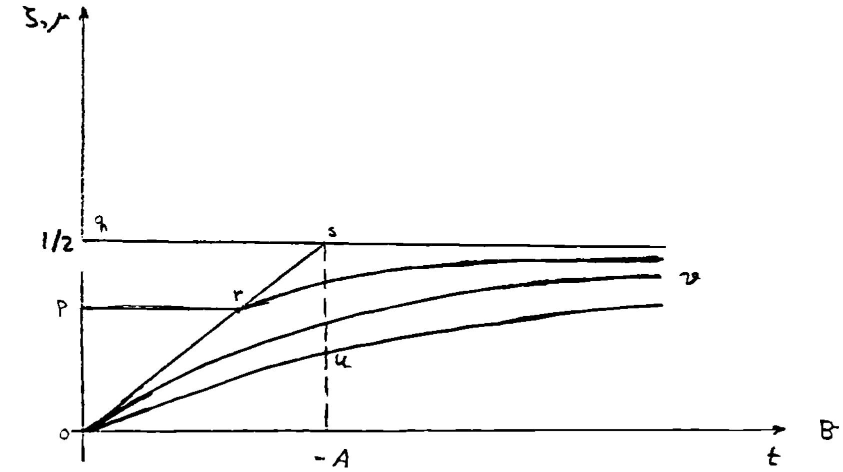

Fig. 8. Isotherms for $J > 0 > A$. qsv: ζ for $kT = 0$. orsv: μ for $kT = 0$. prv: ζ for $0 < kT < J/2$. orv: μ for $0 < kT < J/2$. ov: μ and ζ for $kT = J/2$. ouv: μ and ζ for $kT > J/2$. ot: μ and ζ for $kT \to \infty$.

Figure 9, in which $J, J + A < 0$, shows a transition at zero temperature: for $B > -J - A$, the zero-temperature magnetization is 1/2. For magnetic fields less than that, it is less than 1/2. The magnetization is always parallel to the magnetic field. There is no spontaneous magnetization.

Figure 10, in which $A, J + A > 0$, shows a spontaneous magnetization for $kT < (J + A)/2$. The magnetization is always parallel to the magnetic field.

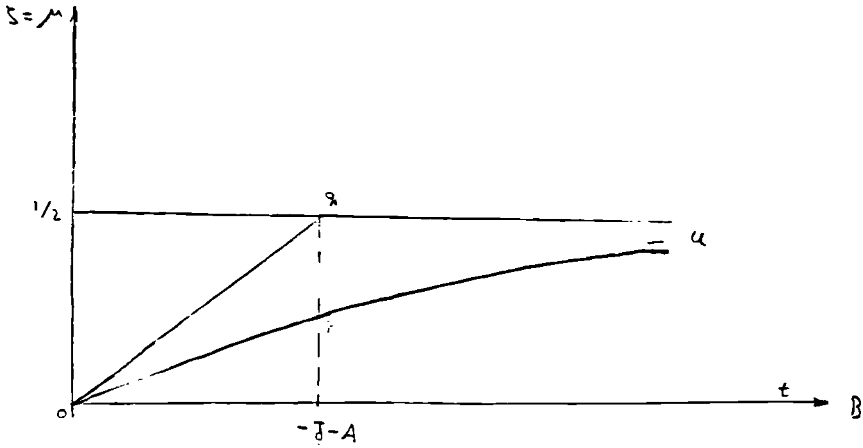

Fig. 9. Isotherms for $J, J + A < 0$. oqu: μ and ζ for $kT = 0$. ou: μ and ζ for $0 < kT$. ot: μ and ζ for $kT \to \infty$.

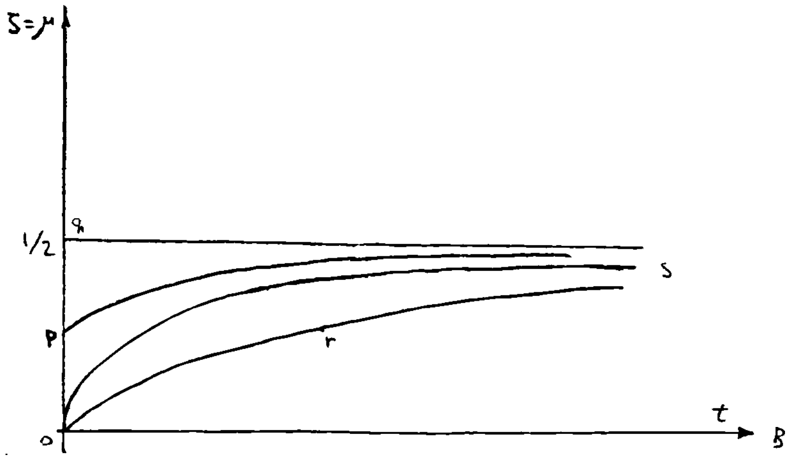

Fig. 10. Isotherms for A, $J + A > 0$. qs: μ and ζ for $kT = 0$. ps: μ and ζ for $0 < kT < (J + A)/2$. os: μ and ζ for $kT = (J + A)/2$. ors: μ and ζ for $kT > (J + A)/2$. ot: μ and ζ for $kT \to \infty$.

REFERENCES

1. D. Faddeev, *Sov. Sci. Rev. C Math. Phys.* **1** (1980), 107.
2. D. Faddeev, Integrable models in 1 + 1 dimensional quantum field theory, in *Les Houches Lectures 1982*, Elsevier, Amsterdam (1984).
3. J. Baxter, *Exactly Solvable Models in Statistical Mechanics*, Academic Press, London (1982).
4. . Calogero; *J. Math. Phys.* **10** (1969), 2191, 2197.
5. . Sutherland, *Phys. Rev. A* **4** (1971), 2019; **5** (1972), 1372.
6. P. Polychronakos, *Phys. Rev. Lett.* **69** (1992), 703.
7. V. Karimipour, *J. Math. Phys.* **39**(1) (1998).